

Numerical Modelling of Deflection of the Flow at the Bucket Splitter of Pelton Turbine

Rupa Pandey^a, Mahesh Chandra Luintel^b

^{a, b} Department of Mechanical and Aerospace Engineering, Pulchowk Campus, IOE, Tribhuvan University, Nepal

✉ ^a rupapandey118@gmail.com, ^b mcluintel@ioe.edu.np

Abstract

Severe erosion of hydro-mechanical parts of hydropower projects (excluding storage type projects) seen in Himalayan-originated rivers is one of the major operational challenges for the hydropower industry. Hydropower facilities in Nepal's young and vulnerable mountainous regions must deal with severe hydro-abrasive erosion of hydraulic components, which lowers efficiency, frequently disrupts power generation, and necessitates downtime for repair or replacement. Parts like nozzles and buckets, which have strong flow acceleration and rapidly changing velocity components, make Pelton turbines susceptible to erosion. In this study, a methodology for modelling the deflection of flow at pelton turbine bucket has been proposed and then used for modelling of the flow in a micro Pelton turbine. The obtained results are compared to theoretical observations as well as to the experimental literature that has already been published. In compared to theoretical calculations, there is a 32.75 % inaccuracy in the thickness of the water sheet and a -11.5 % inaccuracy in the jet velocity.

Keywords

Pelton Turbine, ANSYS Fluent(CFD), Eccentricity, overpressure, water sheet thickness

1. Introduction

In Nepal, there are about 6,000 rivers and rivulets. Due to its unique geography and abundant water supply, Nepal has a wealth of hydropower potential. There is an overall production capacity of 83,000 megawatts (MW) and the economically viable production capacity of roughly 43,000 MW.

The development of hydropower facilities is greatly hampered by the passage of silt particles in rivers. Particularly at high- and medium-head hydroelectric power facilities, the hydro turbines experience erosion due to the abrasive impact of hard particles like quartz and feldspar [1, 2]. According to a forced perspective on the erosion phenomenon in the Pelton bucket, the outer part of the bucket is most vulnerable to erosion because there, the separation forces acting on the sediment particles are greatest [3]. The Pelton bucket experiences the highest erosion since its bottom has the shortest radius of curvature [3]. Due to maintenance expenses and output losses, hydro-abrasive erosion of hydraulic turbines is a problem that has a significant economic impact, especially at high- and medium-head run-off-river

hydropower plants [4].

Hydro turbine selection for a particular site depends upon the head and flow conditions. From the turbine selection nomogram chart one can easily conclude that the Pelton turbine is employed in high head sites [5]. In the young and fragile mountainous areas of Nepal, hydropower plants must contend with significant hydro-abrasive erosion of hydraulic components, which reduces efficiency, causes frequent power generating disruptions, and requires downtime for repair or replacement. A Pelton turbine is prone to erosion because parts like nozzles and buckets have high acceleration of flow and rapidly changing velocity components respectively [5]. Figure 1. presents the list of major hydropower projects in which Pelton turbines are installed in Nepal.

Pelton turbine buckets are mounted on the periphery of the runner. The buckets mounted are either double hemispherical or double ellipsoidal shaped. The first dedicated study about sediment erosion in Pelton turbine is by Bajracharya [6]. Before this, a dedicated study to understand erosion in Pelton turbine nozzles

	S.N	Name of the Project	Total Capacity (in MW)	Unit Capacity (in MW)	Status	Reference
Owned by NEA	1	Kulekhani I	60	30.5	Running	NEA, 2017
	2	Ilam (Puwakhola)	6.2	3.1	Running	NEA, 2017
	3	Sundarjal	0.64	0.32	Running	NEA, 2017
Owned by IPPs	1	Khimtikhola	60	12	Running	IPPAN, 2018
	2	Chilime	22	11	Running	IPPAN, 2018
	3	Chhyangdi	2	1	Running	IPPAN, 2018
	3	Upper Tamakoshi	456	76	Running	IPPAN, 2018
	4	Sanjen	42.5	15	Under Construction	IPPAN, 2018
Total Operating (Running)			606.84			

Figure 1: Major Hydropower Projects with Pelton Turbine

has been least published. Due to development and advancement in Computational Fluid Dynamics (CFD) flow and erosion patterns can now be predicted with computer based numerical simulation. Following the erosion, the runner’s effectiveness is reduced and mechanical vibration is introduced. Therefore, it is necessary to replace the runners on a regular basis to maintain an acceptable degree of vibration and overall generation efficiency. In the case of a Pelton turbine, there is a possibility of eccentricity or mismatch between the needle tip and bucket splitter either during repair and maintenance or during re-installation. Such eccentricity may be either offset type (linear shift of needle center and splitter tip) or angular mismatch between bucket-jet (angle between jet axis and splitter tip being other than 180 Degrees).

Pelton turbines’ bucket splitters are typically designed with an angle 2ϵ of 25 to 40 degrees. It typically takes in the jet at a non-perpendicular angle to both the jet axis and the relative flow rate. For the sake of simplicity, only the scenario where the bucket primary splitter is exactly perpendicular to the jet axis is taken into account here. The flow is abruptly deflected by the angle, which causes a shock strain on the bucket. Shaft power is a result of the corresponding shock load force acting on the moving bucket. Its determination is merely made in accordance with the momentum law.

Recently, numerical models that enable intricate free surface flow simulation have been created and improved. The two main models available in commercially used CFD codes are the mixture model and the volume of fluid (VOF). These models are then widely used for modeling the flow in Pelton turbine

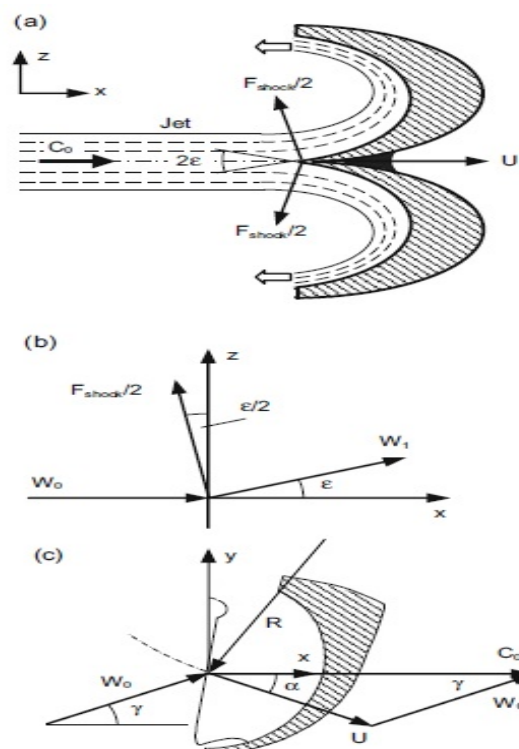


Figure 2: Deflection of flow in splitter (a) with Forces (b) and Flow Components (c) (Adopted from Zhang 2016)

and assembly [7]. The results of study of change in bucket surface keeping inlet and exit angles same as from standard formulation has been published in [7]. The authors have formulated the jet-bucket interaction as steady state flow and evaluated flow across the bucket for different bucket depth. The study of steady state jet and eccentric jet has been published in [5] and [8] respectively. The authors have formulated the jet as steady state and studied properties of jet in different opening of the Nozzle.

Stepping on to the development, this study intends to develop the capacity to model flow in Pelton turbine bucket (jet-bucket interaction). In this study, transient state formulation of jet-bucket interaction is done with intention to study the deflection of the flow at the bucket splitter. The velocity of jet and jet thickness are then computed and compared against theoretical calculations for verification of modelling approach and methodology adopted.

2. Methodology

As shown in figure 3, the study commenced with the development of the CAD model of the flow domain

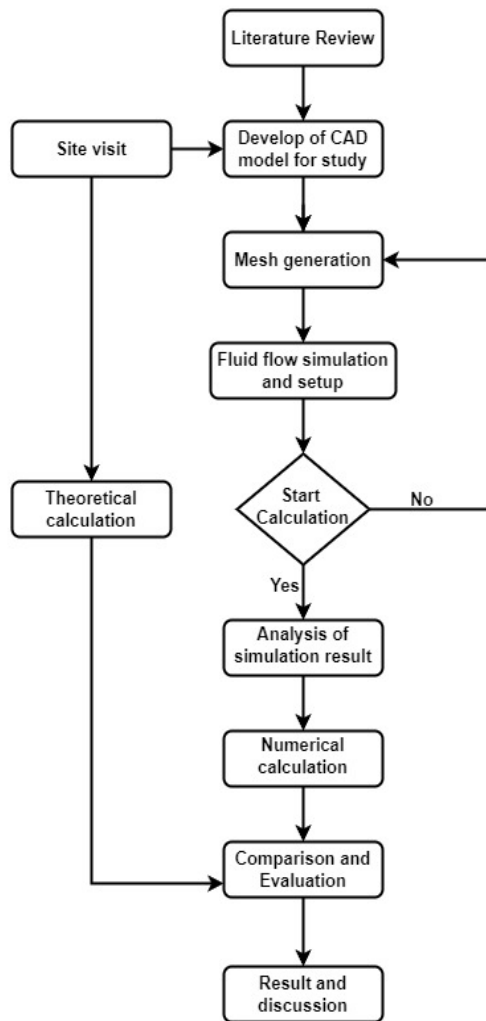


Figure 3: Methodology for Research Work

with intent for modeling the flow. For simplicity, only one half of the bucket has been modeled.

The method adopted for any CFD simulation process is summarized in figure 3

In the CFD simulation flow process shown in Figure 4, the analyst develops a finite element mesh in Pre-processing to divide the subject geometry into subdomains for mathematical analysis and applies material properties and boundary conditions. Boundary conditions information will be used as per (Bajracharya, 2008) [9, 5, 8, 10]. With ANSYS Fluent, the flow in the bucket and jet-bucket interaction will be captured. The results will be obtained for velocity profiles, pressure profiles and water sheet thickness profiles from the simulation in the ANSYS fluent. In this case, to model the flow domain, 3D CAD

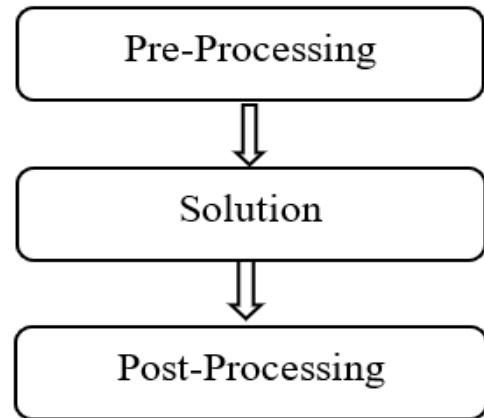


Figure 4: Process Flow of CFD Simulation

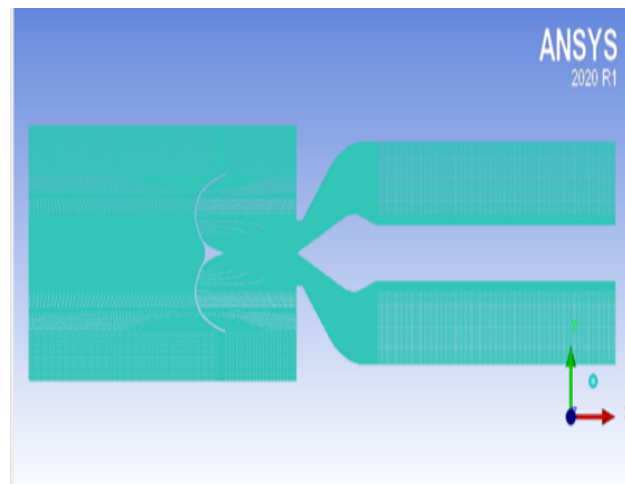


Figure 5: Full Mesh of Bucket Jet

software, CATIA will be used for its ability to better model the surface topology. Better modeling of surface topology is expected to ease us during the mesh generation. As two-dimensional flow simulation will be done, a part of the domain will be modeled. The meshing of the domain will be done by using ICEM CFD 2020 as shown in Figure 5. To capture the viscous layer effects (boundary layer) in fluid flow, the fine mesh will be used near all the flow walls namely, injector walls, nozzle, needle and bucket.

The solution, during which the program derives the governing matrix equations from the model and solves for the primary quantities. Here we will use ANSYS Fluent 2020 for the solution. Fluent is a finite volume-based program that has two solvers i.e., pressure-based and density based. As our problem does not incorporate changes in density, we will use the pressure-based solver. Most commercial codes are now finite volume based. The finite volume method is

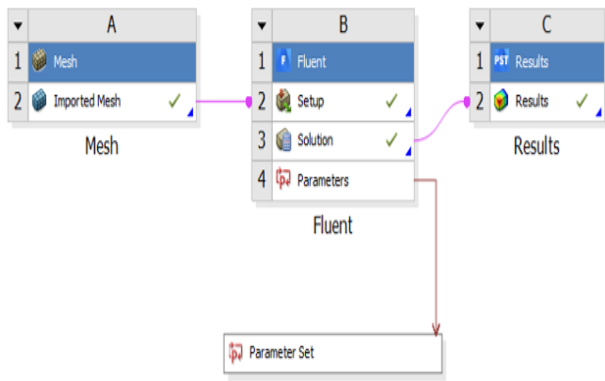


Figure 6: Basic Workflow

easier (or more natural) to implement for unstructured meshes and is more stable. In the ANSYS Fluent processes, series of parameters need to be set the Figure 6 of basic workflow show the steps involvement during the solver settings. Two-Phase Transient State Modeling: Gravity was defined in negative y-axis (i.e -9.8 m/s^2). Turbulence model used was a realizable k-epsilon model based on past practice and as recommended by the ANSYS Fluent theory guide for multiphase flow simulation for jet flows. The VOF model was employed with primary fluid assigned to air and secondary fluid was set to water with the surface tension coefficient set to 0.072 N/m, and the surface tension model was continuum surface force. The second order discretization scheme was chosen and as recommended by ANSYS Fluent theory guide, default transient scheme, second order backward Euler was chosen. To trace the interface of water and air, the geo-reconstruct scheme was employed. Residuals are important for they measure convergence, for all governing equations 0.0001. As regards boundary conditions, the inlet was defined as a pressure inlet condition with the numerical value set to 3 bar, the outlet was set to one atmosphere. For multiphase simulation, at the inlet, the value of the water phase was set to 1 and the value of air was set to 0. For the rest of the nodes across the domain, the velocity was initialized to 1.5 m/s, pressure to 3 bar, and air volume fraction as 1.

the analyst checks the validity of the solution in Post-processing and examines the values of primary quantities (such as displacements and stresses) and derives and examines additional quantities (such as specialized stresses and error indicators). An inbuilt program in ANSYS Workbench CFD Post shall be used for post-processing the CFD results.

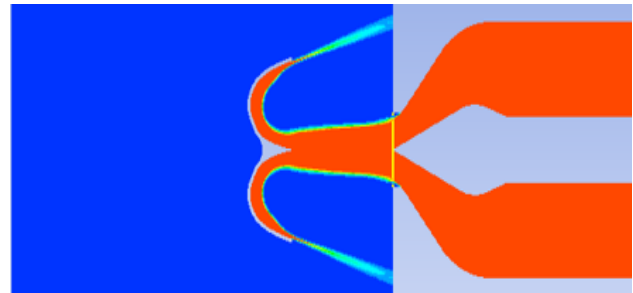


Figure 7: Region of Interest (Indicated by a yellow Line at Needle Tip)

3. Result and Discussion

The transient state simulation was performed with an implicit VOF scheme and with a Geo-reconstruct scheme for identifying the air-water interface. The Geo-reconstruct scheme tracks the interface between two fluids based on the geometrical information. It is claimed to be the most accurate scheme to track interface by ANSYS Fluent Theory Guide but takes a relatively larger computation time. The scheme was successful to meet the target residual of 0.0001 within a maximum of 100 iterations for each time step update. Total simulation time was 100 CPU hours for the implicit scheme to get the desired type of solver settings.

3.1 Velocity Profile for Centric Placement

For verification of the current adopted numerical modeling, a comparison of velocity profile with experimentally measured value was done.

From figure 8, it can be seen that the velocity profile at the Needle tip is zero, which is as desired and matches with previous findings of [5, 8, 10]. The maximum velocity is computed by custom calculation expression using an inbuilt function in CFD Post.

3.1.1 Error Calculation

The error as calculated in Figure 9 is accounted for the fact that, though the design has been done for maximum efficiency conditions, the jet constant, which is calculated to be 0.5 for maximum efficiency conditions may not be achieved on same jet constant because of some errors during manufacturing and instrumentation. In addition, there are errors present in Numerical simulation which are systematic.

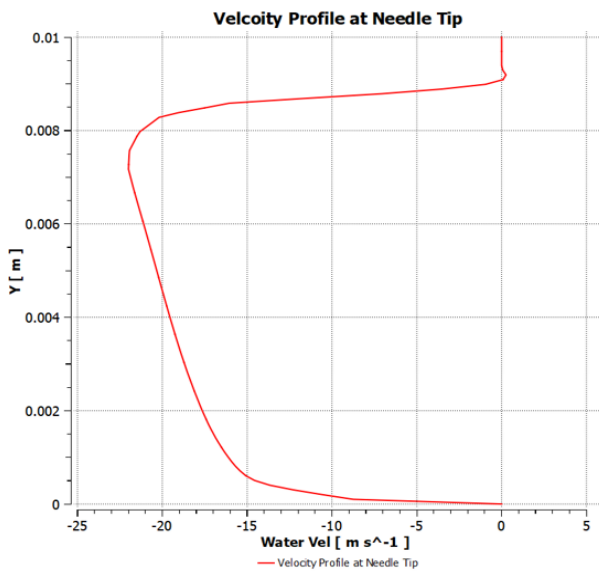


Figure 8: Velocity (X-Velocity) Profile at Needle Tip (Upper Half Only)

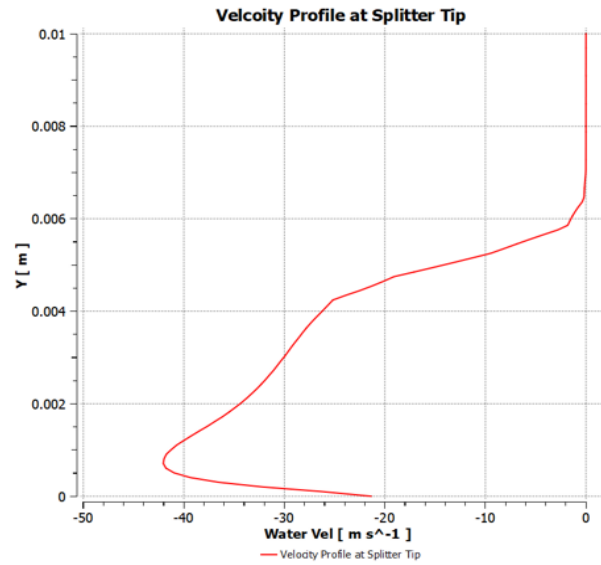


Figure 11: Velocity Profile at Splitter Tip (Upper Half Only)

Calculation of Jet Velocity (Experiment)			
S.N.	Item	Value	Units
1	Runner PCD	0.175	m
2	Measured Runner RPM	1430	RPM
3	The linear speed of Bucket	13.10	m/s
4	Assuming maximum eff. Condition, Jet Velocity	26.21	
Error analysis			
<i>Velocity from Computations as measured at the location of runner bucket, the point where Jet and Bucket Interact</i>			
1	X- Velocity (Absolute)	21.99	m/s
	<i>Error in Computation</i>	-16.08%	
1	Resultant Velocity (Absolute)	23.219	m/s
	<i>Error in Computation</i>	-11.5%	

Figure 9: Experimental reading and error calculation

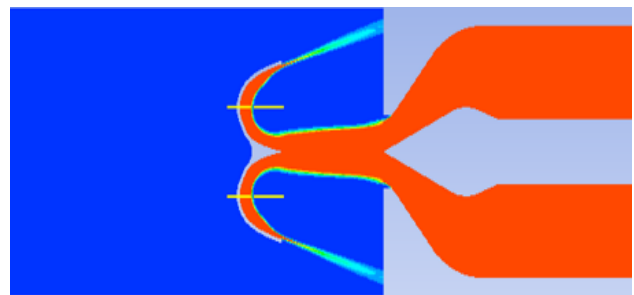


Figure 12: Region of Interest (Indicated by a yellow Line at Bucket Center)

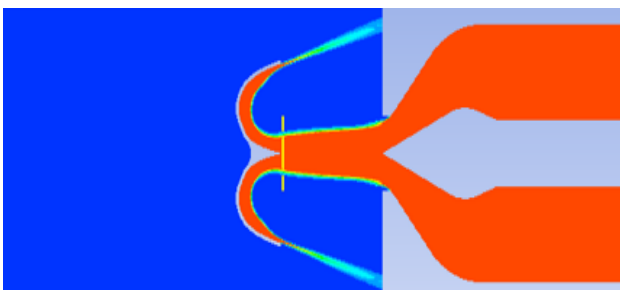


Figure 10: Region of Interest (Indicated by a yellow Line at Splitter Tip)

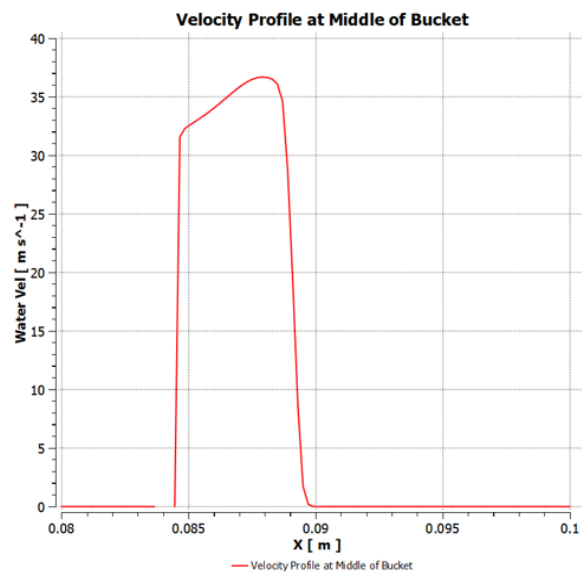


Figure 13: Velocity Profile at Bucket Mid

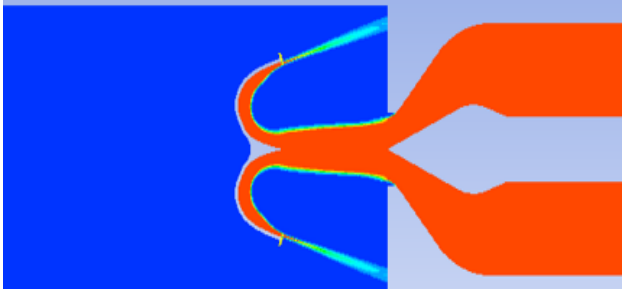


Figure 14: Region of Interest (Indicated by a yellow Line at Bucket Exit)

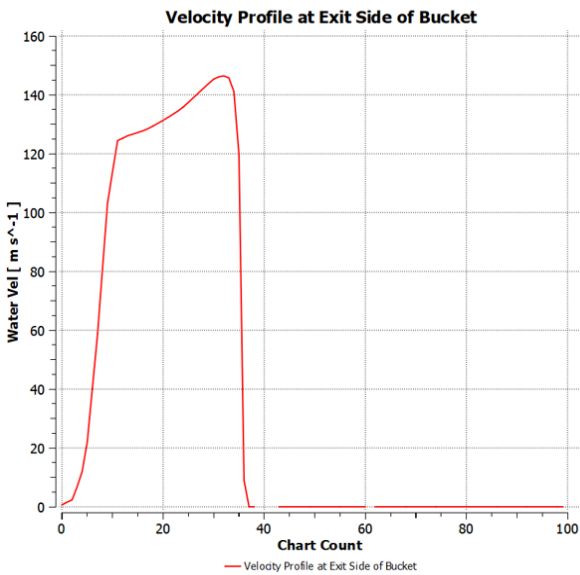


Figure 15: Velocity profile at Exit

The distribution of water flow in the bucket after the achievement of the steady-state flow with the region of interest indicating by yellow line in different position as shown in Figure 7, Figure 10, Figure 12 and Figure 14.

From the velocity profile of splitter shown in Figure 11 indicates the higher velocity at the splitter tip and graph show that the as height increases velocity decreases. The zero value of Figure 13 corresponds to the position of bucket mid for non-eccentric case and increase the velocity towards the positive axial direction from mid of the bucket. when the water leave the bucket the velocity at the exit condition seen in Figure 15 has been higher for certain distance and decreases to zero value as flow continue to move in the positive axial direction.

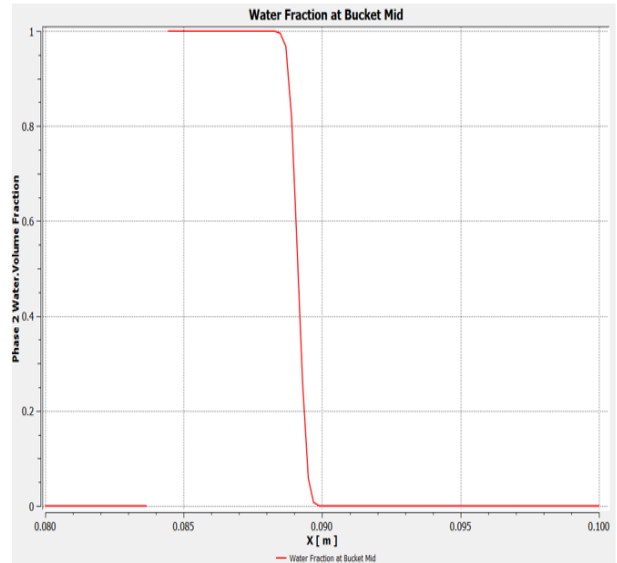


Figure 16: Water Volume Fraction

3.2 Water Sheet Thickness during Normal Installation

The water-sheet width in the bucket can be assumed to linearly increase with the distance covered by the flow. At the bucket entry, the water-sheet width is equal to the jet diameter (d_1). At the bucket exit, it can be assumed to be 85% of the bucket width B at the nominal flow rate. The water-sheet height h along the sheet width d can be assumed to be uniform and thus constant [11]. The expression of water sheet height at the bucket,

$$h = 0.05 * B \tag{1}$$

The water-sheet height h along the sheet width d can be assumed to be uniform and thus constant. The expression of water sheet height at the bucket,

$$\begin{aligned} h &= 0.05 * B \tag{2} \\ &= 0.05 * 48.661 \text{ mm} \\ &= 2.433 \text{ mm} \end{aligned}$$

From numerical results as shown in Figure 18, we can get the range for water sheet thickness (From the X-axis) for the volume fraction of water equal to 1 which is 3.23 mm.

Error Calculation:

$$\begin{aligned} \text{error} &= (\text{Numerical value} - \text{Theoretical value}) / (\text{Theoretical value}) \\ &= (3.23 - 2.43305) / 2.43305 \\ &= 32.755\% \end{aligned}$$

Figure 16 shows the water volume fraction values in the inner surface of the bucket at the pitch circle diameter. It was observed that the maximum water sheet thickness was at the middle of the bucket where the curvature area was maximum due to which dispersed flow trap more in the middle of the bucket.

4. Conclusion

In this Study, the flow analysis on Pelton turbine bucket was done using computational fluid dynamics solver and the results obtained are compared with theoretical observations as well as with the previously published experimental literature. This work proposes a methodology for simulating the deflection of flow at the bucket of a Pelton turbine, which is subsequently applied to simulating the flow in a micro Pelton turbine. Results of velocity profile, water sheet thickness, pressure profile were plotted at different locations. The velocity profile obtained from CFD modeling shows zero velocity at needle tip and gradually increases as the flow get dispersed around the bucket with increases of water sheet. The resulting results are contrasted with theoretical predictions as well as previously reported experimental literature. By computational results, the water sheet thickness is estimated 32.75 % more while the jet velocity is estimated less by 11.5 % when compared to theoretical estimate. The error may be due to the mesh sizing, theoretical assumptions in deriving the empirical equations, consideration of bucket as stationary domain in numerical modeling, viscous friction of water sheet in bucket flow and deviation of bucket shape. This method proposed can be employed to model flow in case of altered bucket profile to know effect of alteration in flow pattern.

In this study, deflection of flow at the splitter tip was studied for the case of a 2 kW Pelton turbine unit. Studying the deflection of flow at the splitter tip of large Pelton turbines can also be done using the method utilized in this study, the implicit formulation of the VOF scheme. It is anticipated that the error calculated in this study will be further reduced in the case of large Pelton turbines because the equations of flow deviation employed in this study were developed for the case of larger Pelton turbines. Additionally, adopting a finer mesh and a more thorough theoretical derivation of the equation for calculating water sheet thickness might reduce factors that contribute to the

overall error in Numerical modeling and theoretical formulations. By adopting an explicit VOF formulation, this study may be furthered.

References

- [1] Saurabh Sangal, Mukesh Kumar Singhal, and RP Saini. Hydro-abrasive erosion in hydro turbines: a review. *International Journal of Green Energy*, 15(4):232–253, 2018.
- [2] Laxman Poudel, Bhola Thapa, Bim Prasad Shrestha, Biraj Singh Thapa, KP Shrestha, and NK Shrestha. Computational and experimental study of effects of sediment shape on erosion of hydraulic turbines. In *IOP Conference Series: Earth and Environmental Science*, volume 15, page 032054. IOP Publishing, 2012.
- [3] Anant Kumar Rai, Arun Kumar, and Thomas Staubli. Analytical modelling and mechanism of hydro-abrasive erosion in pelton buckets. *Wear*, 436:203003, 2019.
- [4] David Felix, Ismail Albayrak, André Abgotsson, and RM Boes. Hydro-abrasive erosion of hydraulic turbines caused by sediment—a century of research and development. In *IOP Conference Series: Earth and Environmental Science*, volume 49, page 122001. IOP Publishing, 2016.
- [5] Tri Ratna Bajracharya, Rajendra Shrestha, and Ashesh Babu Timilsina. A methodology for modelling of steady state flow in pelton turbine injectors. *Journal of the Institute of Engineering*, 15(2):246–255, 2019.
- [6] TR Bajracharya. Efficiency deterioration in pelton turbines due to sand-particle-led bucket erosion. *Tribhuvan University*, 2007.
- [7] Neeraj Adhikari, Anup Pandey, Anushka Subedi, and Nitesh Subedi. Design of pelton turbine and bucket surface using non-uniform rational basis spline and its analysis with computational fluid dynamics. *Journal of the Institute of Engineering*, 16(1):41–50, 2021.
- [8] Tri Ratna Bajracharya, Ashesh Babu Timilsina, Anil Sapkota, Tejendra Rahadi Magar, Sameep Shrestha, Tejaswi Sapkota, and Nawaraj Shrestha. Effect of spear needle eccentricity on the pelton turbine jet. In *Proceedings of 9th IOE Graduate Conference*, volume 9, pages 302–309. 9th IOE Graduate Conference Organizing Committee, 2021.
- [9] TR Bajracharya, B Acharya, CB Joshi, RP Saini, and OG Dahlhaug. Sand erosion of pelton turbine nozzles and buckets: A case study of chilime hydropower plant. *Wear*, 264(3-4):177–184, 2008.
- [10] Tri Ratna Bajracharya, Rajendra Shrestha, Anil Sapkota, and Ashesh Babu Timilsina. Modelling of hydroabrasive erosion in pelton turbine injector. *International Journal of Rotating Machinery*, 2022(1):15, 2022.
- [11] Zh Zhang. Working principle of pelton turbines. In *Pelton Turbines*, pages 13–28. Springer, 2016.